THE JOURNAL OF PHYSICAL CHEMISTRY A

Article

pubs.acs.org/JPCA

# Gas Phase Production and Loss of Isoprene Epoxydiols

Kelvin H. Bates,*[,†] John D. Crounse,[‡] Jason M. St. Clair,[‡] Nathan B. Bennett,[†,∥] Tran B. Nguyen,[‡] John H. Seinfeld,[†,§] Brian M. Stoltz,[†] and Paul O. Wennberg[‡,§]

[†]Division of Chemistry and Chemical Engineering, California Institute of Technology, 1200 East California Boulevard, Pasadena, California 91125, United States

[‡]Division of Geological and Planetary Sciences, California Institute of Technology, 1200 East California Boulevard, Pasadena, California 91125, United States

[§]Division of Engineering and Applied Science, California Institute of Technology, 1200 East California Boulevard, Pasadena, California 91125, United States

Supporting Information

**ABSTRACT:** Isoprene epoxydiols (IEPOX) form in high yields from the OH-initiated oxidation of isoprene under low-NO conditions. These compounds contribute significantly to secondary organic aerosol formation. Their gas-phase chemistry has, however, remained largely unexplored. In this study, we characterize the formation of IEPOX isomers from the oxidation of isoprene by OH. We find that *cis-β-* and *trans-β*-IEPOX are the dominant isomers produced, and that they are created in an approximate ratio of 1:2 from the low-NO oxidation of isoprene. Three isomers of IEPOX, including *cis-β-* and *trans-β*, were synthesized and oxidized by OH in environmental chambers under high- and low-NO conditions. We find that IEPOX reacts with OH at 299 K with rate coefficients of $(0.84 \pm 0.07) \times 10^{-11}$, $(1.52 \pm 0.07) \times 10^{-11}$, and $(0.98 \pm 0.05) \times 10^{-11}$ cm$^3$ molecule$^{-1}$ s$^{-1}$ for the $\delta$1, *cis-β*, and *trans-β* isomers. Finally, yields of the first-generation products of IEPOX + OH oxidation were measured, and a new mechanism of IEPOX oxidation is proposed here to account for the observed products. The substantial yield of glyoxal and methylglyoxal from IEPOX oxidation may help explain elevated levels of those compounds observed in low-NO environments with high isoprene emissions.

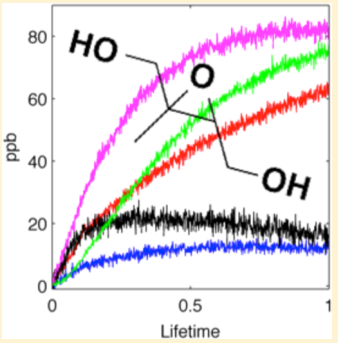


## INTRODUCTION

Isoprene, a volatile organic compound (VOC) produced by deciduous plants, comprises the single most abundant atmospheric nonmethane hydrocarbon by emission to the atmosphere, with estimates near 500 Tg C y$^{-1}$.[1] The rapid oxidation of isoprene by OH radicals ($k = 1.0 \times 10^{-10}$ cm$^3$ molecule$^{-1}$ s$^{-1}$)[2] makes it an important driver in tropospheric chemistry, particularly in forested regions. When NO concentrations are sufficiently low, as is the case in many areas with high isoprene emissions, isoprene oxidation can proceed by a HO$_x$-mediated (OH + HO$_2$) mechanism, which until recently was largely unexplored.[3−5] OH addition to isoprene, followed by O$_2$ addition and the subsequent peroxy radical + HO$_2$ reaction, leads to formation of isoprene hydroxyhydroperoxide (ISOPOOH) in yields exceeding 70%,[6−8] with approximately 2.5% forming methacrolein (MACR) and 3.8% forming methylvinylketone (MVK).[9,10]

Paulot et al.[11] showed that the reaction of ISOPOOH with OH forms isoprene epoxydiols (IEPOX) in yields exceeding 75% (Figure 1). The oxidation mechanism regenerates one equivalent of OH, partially accounting for the stability of HO$_x$ levels observed in remote forested regions.[7,8,11,12] IEPOX formation contributes to secondary organic aerosol (SOA) formation from low-NO$_x$ isoprene oxidation, as its low volatility and high water solubility allow it to partition into the condensed phase.[13−16] Uptake of IEPOX onto acidic aerosol has been shown to contribute significantly to SOA in forested areas where anthropogenic pollutants (e.g., SO$_2$) are present.[17] Estimates of global isoprene oxidation show that 95 ± 45 Tg C of IEPOX per year is formed globally, with the implication that the products of its subsequent reactions play a crucial role in tropospheric chemistry.[11]

Here, we report the relative yield of IEPOX isomers from isoprene oxidation, as well as the rate coefficients and products of their oxidation by OH. Using existing procedures with one significant novel enhancement, three isomers of IEPOX were synthesized. We then performed a series of individual experiments in which IEPOX isomers were oxidized by OH in an environmental chamber. Reaction rate coefficients of the IEPOX isomers were measured relative to propene. The lifetimes of $\delta$1-, *cis-β-*, and *trans-β*-IEPOX against oxidation by OH (at 299 K and [OH] = $1.0 \times 10^6$ molecules cm$^{-3}$, a typical atmospheric value) were found to be 33, 18, and 28 h, respectively. By comparing the isomers' retention times in a gas chromatograph (GC) connected to a chemical ionization mass spectrometer (CIMS) with that of IEPOX formed in situ by low-NO oxidation of isoprene, we show that *cis-β-* and *trans-β*-IEPOX account for the majority of IEPOX produced in the

**Received:** November 1, 2013
**Revised:** January 28, 2014

   dx.doi.org/10.1021/jp4107958 | J. Phys. Chem. A XXXX, XXX, XXX−XXX

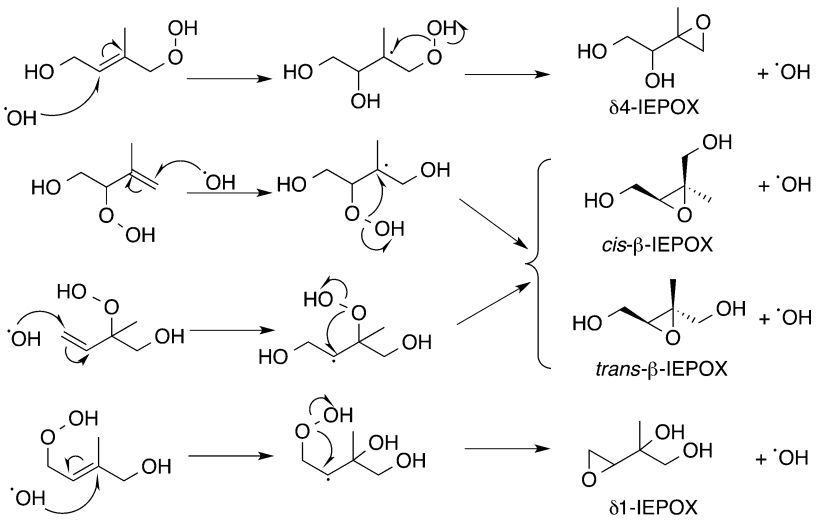


**Figure 1.** Mechanism for the formation of IEPOX from OH-initiated oxidation of ISOPOOH.

atmosphere, while the yield of $\delta$1-IEPOX is small (<3%). These isomer ratios are consistent with the relative concentrations of their hydrolysis products (2-methylerythritol and 2-methylthreitol) observed in ambient aerosol.[17−22] Additionally, experiments in the absence of propene were performed to determine the products of IEPOX oxidation by OH. Previous studies[23,24] have inferred the products by a combination of theoretical models, observations of low-NO isoprene oxidation, and targeted chamber studies on IEPOX analogues. A more recent study[25] measured the products of $\delta$4- and *trans*-$\beta$-IEPOX oxidation by OH. We observed a number of compound masses consistent with products predicted or detected in previous studies, for which we propose oxidative mechanisms. Differences in product yields between high- and low-NO conditions and between IEPOX isomers are described.

## EXPERIMENTAL METHODS

**Synthesis.** The IEPOX isomers used in these experiments were synthesized according to the procedures described by Zhang et al.[26] with one significant change described below. All chemicals were purchased from Sigma Aldrich. The $\delta$1- and *cis*-$\beta$-IEPOX used in photochemical oxidation experiments were 99% pure, as determined by NMR; the *trans*-$\beta$-IEPOX was >92% pure, and the impurity was not found to interfere with any part of the experiments.

Briefly, $\delta$1-IEPOX (2-(oxiran-2-yl)-propane-1,2-diol) was prepared from 2-methyl-2-vinyloxirane (**1**) according to Scheme 1. The epoxide in compound **1** (0.98 g, 11.67 mmol) was first converted to the diol (**2**) by treatment with 0.1 M hydrochloric acid (10 mL), and the product was isolated by lyophilysis. The diol was then treated with *meta*-chloroperoxybenzoic acid (*m*CPBA, 4.25 g, 70%, 17.3 mmol) to afford $\delta$1-IEPOX (**3**, 0.23 g, 1.9 mmol, 17% yield). The $^1$H NMR spectrum (Figure S1, Supporting Information) matched previously published spectra.[26]

*cis*-$\beta$-IEPOX (*cis*-2-methyl-2,3-epoxy-1,4-butanediol) was prepared from 3-methylfuran-2(5*H*)-one, which in turn was prepared from citraconic anhydride (**4**) using procedures described by Nefkens et al. (Scheme 2).[27] Briefly, compound **4** (10 mL, 111.26 mmol) was treated with dicyclohexylamine (DCA, 25 mL, 122.4 mmol) in methanol to produce the DCA salt **5** (20.4 g, 62.7 mmol, 56% yield). Compound **5** was then treated with isobutyl chloroformate ($ClCO_2iBu$, 9 mL, 68.9 mmol) followed without purification by sodium borohydride ($NaBH_4$, 5 g, 132 mmol), to afford 3-methylfuran-2(5*H*)-one (**6**, 3.93 g, 40 mmol, 64% yield), which was purified by fractional distillation.

Conversion of compound **6** to 2-methyl-2-butene-1,4-diol (**7**) was adapted from procedures developed by Hoang et al.[28] and was the only major change from Zhang et al.'s procedures. The use of diisobutylaluminum hydride (DIBAL-H) instead of lithium aluminum hydride improved yields from 27% to 83%.

A flame-dried 100 mL round-bottom flask equipped with a stir bar was charged with compound **6** (1.63 g, 16.6 mmol, 1.00 equiv) and toluene (14 mL, 1.2 M) and lowered into a 0 °C bath (ice/water). DIBAL-H (neat, 4 mL, 22.4 mmol, 1.35 equiv) was added dropwise over several minutes. Once the addition was complete, the bath was removed, and the reaction

**Scheme 1. Reactions in the Synthesis of $\delta$1-IEPOX**

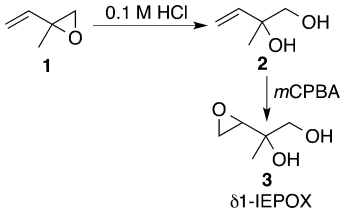


**Scheme 2. Reactions in the Synthesis of *cis*-$\beta$-IEPOX**

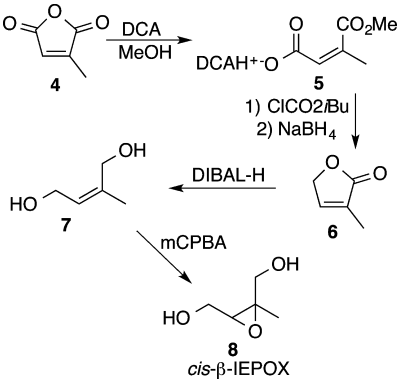



dx.doi.org/10.1021/jp4107958 | J. Phys. Chem. A XXXX, XXX, XXX−XXX

**Scheme 3. Reactions in the Synthesis of *trans*-β-IEPOX**

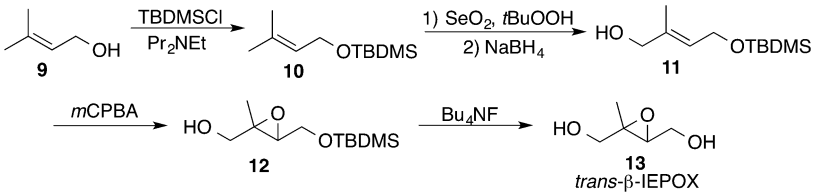


was allowed to warm to room temperature. An additional portion of DIBAL-H (2.2 mL, 12.3 mmol, 0.74 equiv) was added after 1.5 h. TLC analysis at 3 h indicated no remaining starting material. Consequently, the reaction was lowered into a 0 °C bath and quenched with the dropwise addition of methanol (9 mL). The resulting mixture was diluted with toluene (14 mL) and water (3 mL), generating a large amount of solid that was broken up with a spatula. After 1.5 h of stirring, the reaction mixture developed into a biphasic suspension with no significant solids. $MgSO_4$ was added to the flask, and the reaction contents were filtered through a celite/$MgSO_4$ column eluting with MeOH. The resulting organics were concentrated under reduced pressure, generating a white viscous oil. This oil was diluted with ethyl acetate (EtOAc) and again dried over $MgSO_4$, filtered, and concentrated under reduced pressure. The resulting crude oil was purified by flash column chromatography ($SiO_2$, 28 × 2 cm, 20% EtOAc in hexanes → 100% EtOAc) to afford compound **7** (1.40 g, 13.7 mmol, 83% yield) as a pale yellow oil. Compound **7** (0.33 g, 3.35 mmol) was treated with *m*CPBA (2.19 g, 77%, 9.8 mmol) according to the procedures of Zhang et al.[26] to give *cis*-β-IEPOX (**8**, 0.16 g, 1.4 mmol, 42% yield). The $^1$H NMR spectrum (Figure S2, Supporting Information) matched previously published spectra.[26]

*trans*-β-IEPOX (*trans*-2-methyl-2,3-epoxybutane-1,4-diol) was also prepared using procedures published by Zhang et al. (Scheme 3).[26] Briefly, 3-methyl-2-buten-1-ol (**9**, 4.7 g, 54.3 mmol) was treated with *tert*-butyldimethylchlorosilane (TBDMSCl, 9.9 g, 65.7 mmol) and diisopropylethylamine ($Pr_2NEt$, 10.5 mL, 60.3 mmol) to give compound **10** (7.92 g, 39.6 mmol, 73% yield). A hydroxyl group was added to compound **10** in the *trans* position by treatment with selenium dioxide ($SeO_2$, 2.38 g, 21.5 mmol) and *tert*-butylhydroperoxide (*t*-BuOOH, 5.5 M in decanes, 8 mL, 44 mmol) followed without purification by reduction with sodium borohydride ($NaBH_4$, 1.36 g, 36 mmol) to give compound **11** (3.36 g, 15.5 mmol, 39% yield). Epoxidation with *m*CPBA (6.04 g, 77%, 27 mmol) yielded compound **12** (1.51 g, 6.5 mmol, 42% yield), and deprotection with tetrabutylammonium fluoride ($Bu_4NF$, 1 M in THF, 13.5 mmol) gave *trans*-β-IEPOX (**13**, 703 mg, 5.96 mmol, 92% yield). The $^1$H NMR spectrum (Figure S3, Supporting Information) matched previously published spectra.[26]

**Gas Phase Experiments.** Instruments and experimental procedures for gas-phase OH oxidation have been described in detail elsewhere.[23] Briefly, experiments were performed in a 0.85 $m^3$ fluorinated ethylene propylene copolymer (Teflon-FEP, Dupont) chamber at 299 K (±2 K). Hydrogen peroxide ($H_2O_2$), at an initial mixing ratio of 2.5 ppm (±10%), provided the source of $HO_x$ for oxidation upon photolysis under UV lights. Each IEPOX isomer was oxidized in both high- and low-NO conditions (those in which the isoprene peroxy radicals react preferentially with NO or $HO_2$, respectively) with 570 ppb NO added for high-NO oxidation. Propene (125 ppb) provided the internal standard for OH concentration in experiments to determine the oxidation rate coefficient; in product studies, no propene was added.

The chamber was flushed with dry air and evacuated at least four times between successive experiments. In each experiment, IEPOX (30 ppb ±50%, as measured by CIMS) was added to the chamber by spreading a single drop of the compound on the interior surface of a small glass cylinder and passing dry air through the cylinder into the chamber at 20 std L $min^{-1}$. The addition of δ1-IEPOX took 5 min per experiment; the addition of *cis*-β- and *trans*-β-IEPOX took 30 min, and for *cis*-β-IEPOX, the glass cylinder was heated to 60 °C in a water bath during addition to increase volatility. $H_2O_2$ (~8.0 mg, 30% m/m in water) was added by the same method, for 10 min without heating. Propene gas was added by evacuating a 500 $cm^3$ glass bulb and filling it to ~11 Torr with propene, after which the bulb was back-flushed with $N_2$ to atmospheric pressure and pumped down to 11 Torr again. The contents were then flushed into the chamber by passing dry air through the bulb at 20 std L $min^{-1}$ for 1 min. NO was added similarly, by filling the evacuated bulb to ~370 Torr with 1994 ± 20 ppm NO in $N_2$ and flushing the contents into the chamber for 1 min at 20 std L $min^{-1}$.

The chamber's contents were monitored throughout the experiment through a single sample line connected to five instruments: a time-of-flight chemical ionization mass spectrometer (ToF-CIMS, Tofwerk/Caltech); a triple quadrupole MS−MS CIMS (Varian/Caltech); a gas chromatograph with a flame-ionization detector (GC-FID Agilent 5890 II) to measure propene concentrations; a $NO_x$ Monitor (Teledyne 200 EU); and an $O_3$ monitor (Teledyne 400E). Both CIMS systems, which use $CF_3O^-$ as the chemical ionization reagent gas, have been described in detail elsewhere.[23,29,30]

Throughout the experiments, the ToF-CIMS monitored all *m*/*z* between 50 and 340 in negative-ion mode, while the MS−MS CIMS switched between scanning MS mode and tandem MS mode, to detect the fragmentation of IEPOX and its products and to resolve products of isobaric masses. All *m*/*z* signals were normalized to the reagent anion signal. IEPOX was monitored at *m*/*z* 203 (IEPOX + $CF_3O^-$) on both CIMS instruments and by *m*/*z* 203 → *m*/*z* 183 (IEPOX + $CF_3O^-$−HF) on the MS−MS CIMS in tandem MS mode. Photooxidation lasted approximately 3−7 h in each experiment. Nine gas-phase photooxidation experiments were performed, along with two experiments without oxidation to monitor loss of IEPOX to surfaces; details of the experiments are shown in Table 1.

Before and after photooxidation, monitoring by the five instruments described above was interrupted to separate compounds by gas chromatography before sampling by ToF-CIMS (GC-CIMS). One to three GC-CIMS runs were performed before and after each experiment. In each run, approximately 200 $cm^3$ of gas sample was cryo-collected on the head of an RTX 1701 column (Restek) submerged in


dx.doi.org/10.1021/jp4107958 | J. Phys. Chem. A XXXX, XXX, XXX−XXX

**Table 1. Gas Phase IEPOX Experiments**

| run | IEPOX isomer | NO (ppbv) | propene (ppbv) | duration of photooxidation | objective |
|---|---|---|---|---|---|
| 1 | *cis-β* | 571 | 125 | 4:54:10 | OH rate |
| 2 | *cis-β* | 0 | 124 | 6:08:40 | OH rate |
| 3 | *cis-β* | 0 | 0 | | wall loss |
| 4 | *δ*1 | 0 | 126 | 5:58:30 | OH rate |
| 5 | *δ*1 | 563 | 123 | 3:13:00 | OH rate |
| 6 | *cis-β* | 0 | 0 | | wall loss |
| 7 | *cis-β* | 0 | 0 | 6:59:30 | products |
| 8 | *cis-β* | 570 | 0 | 7:01:30 | products |
| 9 | *trans-β* | 0 | 124 | 4:00:00 | OH rate |
| 10 | *trans-β* | 568 | 124 | 4:00:00 | OH rate |
| 11 | *trans-β* | 567 | 0 | 4:30:00 | products |

isopropanol chilled with liquid nitrogen (249 ± 3 K). The isopropanol bath was removed, and the column was allowed to warm for 60 s before the GC temperature program was started (30 °C for 0.1 min, +3 °C/min to 60 °C, +10 °C/min to 130 °C, hold 3 min). Compounds eluted from the GC were ionized by $CF_3O^-$ and monitored between $m/z$ 50 and 340 at a time resolution of 10 $s^{-1}$. Transmission through the GC varied between 60% and 70% for both IEPOX isomers and was not significantly different between the isomers. Further details regarding the GC-CIMS methodology will be provided in a forthcoming manuscript.

**Determination of CIMS Sensitivity to IEPOX.** The CIMS sensitivity to IEPOX was determined in four experiments, two each for *cis-β*- and *trans-β*-IEPOX, performed in the larger (24 $m^3$) Caltech environmental chamber. In each experiment, dilute (1−3 mM) aqueous solutions containing one IEPOX isomer and hydroxyacetone (as an internal standard) were atomized into the Teflon-FEP chamber for 2−8 h through a 15 cm perfluoroalkoxy Teflon transfer line. Temperature was ramped from 35 to 45 °C over the course of atomization to ensure minimal condensational losses. The measured weight of solution atomized allowed quantification of the moles in the chamber. During atomization, the mixing ratio of gas-phase IEPOX was monitored by $CF_3O^-$ negative-ion CIMS with a Varian triple quadrupole mass analyzer, described in greater detail elsewhere.[29] The instrument operated at 26.6 Torr and switched between scanning MS mode ($m/z$ 50−250) and tandem MS mode, with unit mass resolution and 2−5 min time resolution. Dividing the CIMS normalized counts at $m/z$ 203 (scanning MS mode) by the moles of IEPOX in the gas phase provided an estimate of the CIMS sensitivity. The dependence of IEPOX sensitivity on humidity was measured by adding various mixing ratios of water vapor to the CIMS during IEPOX detection. No humidity dependence was detected. We find that the *cis-β*-IEPOX sensitivity is 1.8 times that of *trans-β*-IEPOX, consistent with the previously calculated ion−molecule collision rate ratio of 1.61 to 1 based on polarizability and dipole moments.[11]

**Wall Loss Experiments.** Experiments were performed in both the 0.85 and 24 $m^3$ chambers to determine the extent to which the decay of IEPOX concentration with time could be attributed to loss to chamber walls. In both chambers, wall loss of IEPOX (~0.4% $h^{-1}$) was negligible compared to either loss by photooxidation or signal fluctuations due to temperature, except when nitric acid was injected to acidify the walls in the small chamber. The dramatic loss under acidic conditions is expected based on the sensitivity of the epoxide group in IEPOX to acid. Wall losses were accounted for in subsequent calculations of IEPOX photooxidation rates and products.

## RESULTS AND DISCUSSION

**IEPOX + OH Rate Coefficients.** Rate coefficients for the reaction of each IEPOX isomer with OH were calculated relative to that of propene with OH, for which the rate coefficient is well characterized; the value used in these calculations was $2.62 \times 10^{-12}$ $cm^3$ $molecule^{-1}$ $s^{-1}$ at 299 K.[31] A linear regression analysis of the natural log of the IEPOX concentration (normalized to the initial concentration) versus time over the course of photooxidation (Figure 2) gives a slope

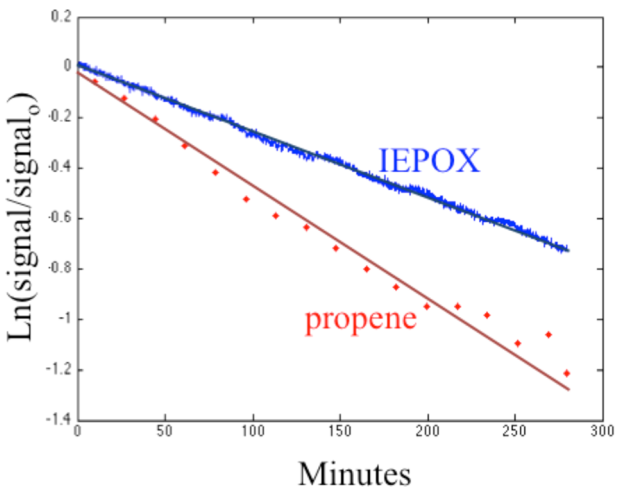


**Figure 2.** Decay of *cis-β*-IEPOX and propene in Exp. 1. The ratio of the slopes of propene and IEPOX concentrations over time (both on logarithmic scales) is equal to the ratio of the rate constants of each species' reaction with OH. Propene data are from GC-FID, while IEPOX data are from ToF-CIMS measured at $m/z$ 203.

equal to the rate coefficient, $k$, multiplied by the concentration of OH. A similar regression can be performed for propene. The ratio of the two slopes is thus equal to the ratio of rate coefficients for oxidation of IEPOX and propene by OH, which allows for the calculation of the OH oxidation rate coefficient of IEPOX.

IEPOX + OH rate coefficients were calculated for each experiment with propene (Exp. 1, 2, 4, 5, 9, and 10), which included a high- and low-NO run for each of the three isomers. Propene concentrations were measured by GC-FID, and IEPOX concentrations by ToF-CIMS. Rate coefficients were then calculated using a linear regression method incorporating error in both dimensions, followed by an error-weighted mean[32] of each isomer's runs. Rate coefficients determined in high- and low-NO experiments differed by no more than 19%, and the run-to-run differences did not correlate with NO level. Primary sources of error include fluctuations in temperature, which affect both oxidation rate coefficients and CIMS sensitivity to IEPOX, and the relative precision and frequency of GC-FID propene measurements.

Calculated OH oxidation rate coefficients and lifetimes for the three IEPOX isomers at ambient temperature are given in Table 2, along with the error bounds derived from linear regressions. *cis-β*-IEPOX was found to react significantly faster than *δ*1- or *trans-β*-IEPOX with OH. The rate coefficients range from $(0.84 \pm 0.07) \times 10^{-11}$ $cm^3$ $molecule^{-1}$ $s^{-1}$ to $(1.52 \pm 0.07) \times 10^{-11}$ $cm^3$ $molecule^{-1}$ $s^{-1}$, consistent with the value


dx.doi.org/10.1021/jp4107958 | J. Phys. Chem. A XXXX, XXX, XXX−XXX

**Table 2. Rate Coefficients for the Reaction with OH of δ1-IEPOX, *cis*-β-IEPOX, and *trans*-β-IEPOX**

| isomer | rate ($k$)[a] | low NO[a] | high NO[a] | lifetime[b] |
|---|---|---|---|---|
| δ1 | 0.84 ± 0.07 | 0.97 | 0.82 | 33.0 ± 2.8 |
| *cis*-β | 1.52 ± 0.07 | 1.40 | 1.62 | 18.3 ± 0.8 |
| *trans*-β | 0.98 ± 0.05 | 0.88 | 1.05 | 28.3 ± 1.4 |

[a]In units $\times 10^{-11}$ cm$^3$ molecule$^{-1}$ s$^{-1}$. [b]In units h, for [OH] = $10^6$ molecules cm$^{-3}$.

previously estimated as an upper limit by Paulot et al.[11] of $1.5 \times 10^{-11}$ cm$^3$ molecule$^{-1}$ s$^{-1}$. The only other study to have measured the OH oxidation rate coefficients of specific IEPOX isomers, by Elrod et al.,[25] reported the rate coefficient of δ4-IEPOX + OH to be $(3.52 \pm 0.72) \times 10^{-11}$ cm$^3$ molecule$^{-1}$ s$^{-1}$ and that of *trans*-β-IEPOX + OH to be $(3.60 \pm 0.76) \times 10^{-11}$ cm$^3$ molecule$^{-1}$ s$^{-1}$. These values are significantly higher than those reported here and are inconsistent with the dynamics of the isoprene system studied by Paulot et al.[11] Clearly, further studies will be needed to resolve these differences.

**Relative Yields of IEPOX Isomers.** Comparison of GC retention times of each IEPOX isomer to those of low-NO isoprene oxidation products reveals that *cis*-β- and *trans*-β-IEPOX are produced in much higher yield than δ1-IEPOX in the gas phase oxidation of isoprene by OH. These results are shown in Figure 3, in which $m/z$ 203 ($CF_3O^-$ clustered with IEPOX or ISOPOOH) normalized counts are plotted versus retention time for the three IEPOX isomers and for two oxidation times in the low-NO oxidation of isoprene by OH, conducted under the same conditions as the low-NO IEPOX experiments detailed above. After 1 h, isoprene oxidation forms primarily two isomers of ISOPOOH, which appear on the GC-CIMS $m/z$ 203 trace as two peaks centered at 12.5 and 13.3 min. After 10 h, some ISOPOOH remains, but two IEPOX peaks dominate, centered at 13.9 and 14.4 min. These correspond to *trans*-β- and *cis*-β-IEPOX, respectively. δ1-IEPOX also appears on the oxidized isoprene trace but with a far smaller signal. The ratio of peak areas corresponding to δ1-, *cis*-β-, and *trans*-β-IEPOX is, respectively, 1 to 20.5 to 27.9.

While the CIMS sensitivity of δ1-IEPOX was not directly measured, previous calculations of molecular dipoles have determined that the sensitivity to δ1-IEPOX should be nearly equivalent to that of *cis*-β-IEPOX, and any deviation from this prediction is not expected to outweigh the large difference in peak areas between δ1-IEPOX and the other isomers. Thus, δ1-IEPOX is far less atmospherically relevant than the β-IEPOX isomers. δ4-IEPOX forms by a mechanism similar to that of the δ1 isomer and likely has a similar retention time in the GC due to its analogous structure. No additional peaks were observed near the retention time of δ1-IEPOX that could have been assigned to δ4-IEPOX in the 10 h GC trace. Therefore, the δ4 isomer is expected either not to be formed or to coelute with δ1-IEPOX, in which case the integrated peak area assigned to δ1-IEPOX accounts for the sum of the δ1 and δ4 isomers.

Results from the sensitivity calibrations discussed above show that the single MS CIMS signal at $m/z$ 203 is 1.83 times more sensitive to *cis*-β-IEPOX than *trans*-β-IEPOX. Scaling the GC signal areas by the sensitivity, we find that OH-initiated low-NO oxidation of isoprene produces concentrations of *cis*-β- and *trans*-β-IEPOX after 10 h of oxidation in a ratio of 1 to 2.5 (±0.5). Part of this difference in concentrations can be explained by the faster reaction with OH of *cis*-β-IEPOX relative to *trans*-β-IEPOX. Using a simple kinetic model of isoprene, ISOPOOH, and IEPOX mixing ratios based on the signals observed in the low-NO oxidation of isoprene and the reaction rates calculated in the present study, we find the ratio of the yields of *cis*-β-IEPOX to *trans*-β-IEPOX produced from the reaction of isoprene with OH to be 1 to (2.13 ± 0.30) and that *cis*-β- and *trans*-β-IEPOX together account for >97% of observed IEPOX. The ratio of the *cis* and *trans* yields is similar to the ratio of 2-methyltetrol isomers found in SOA created by oxidation of isoprene by OH. Assuming that particle-phase hydrolysis of IEPOX proceeds by a typical acid-catalyzed mechanism as the evidence suggests,[33] in which protonation of the epoxide is followed by $S_N2$ attack by water, *cis*-β-IEPOX is expected to form 2-methylthreitol, while *trans*-β-IEPOX would form 2-methylerythritol. These 2-methyltetrol isomers have repeatedly been observed in isoprene-generated SOA in ratios of approximately 1 to 2, comparable to the ratio between *cis*- and *trans*-β-IEPOX that we observe.[17−22]

**Gas Phase Products of the Reaction of IEPOX with OH.** Experiments performed in the 0.85 m$^3$ chamber in the absence of propene (Exp. 7, 8, and 11) were used to determine the products of gas-phase OH oxidation of *cis*-β- and *trans*-β-IEPOX. No product studies were performed on δ1-IEPOX due to its low atmospheric relevance. Mixing ratios of oxidation products were determined by multiplying the CIMS signal, normalized to the concentration of reagent ion in the chemical ionization region, by a calibration factor. For small, commercially available compounds, mixing ratio calibration

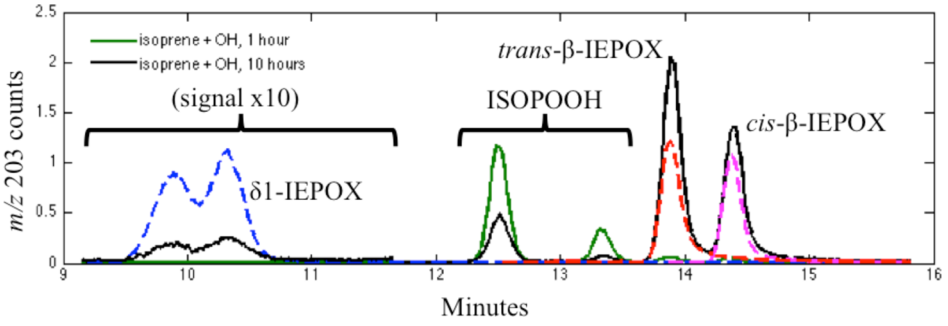


**Figure 3.** CIMS signals at $m/z$ 203 from GC-CIMS chromatograms of δ1-IEPOX (blue), *cis*-β-IEPOX (pink), and *trans*-β-IEPOX (red) synthesized standards, as well as the $m/z$ 203 products from OH-initiated low-$NO_x$ oxidation of isoprene. The two major peaks seen after one hour of isoprene + OH oxidation (green) represent ISOPOOH, while the two major peaks seen after ten hours of oxidation (black) correspond with *cis*-β- and *trans*-β-IEPOX. The 10 h signal is multiplied by a factor of 10 between minutes 9.2 and 11.7, to show that a minor amount of δ1-IEPOX is formed. δ1-IEPOX appears as a double peak because the compound has two diastereomers.


dx.doi.org/10.1021/jp4107958 | J. Phys. Chem. A XXXX, XXX, XXX−XXX

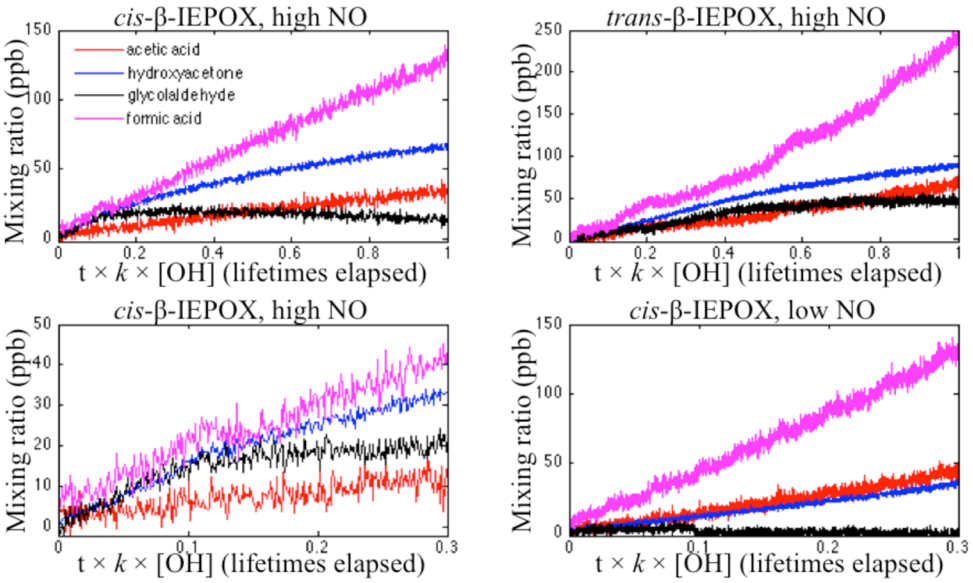


**Figure 4.** Time traces of dominant small products observed in the OH-initiated oxidation of *cis-β-* and *trans-β*-IEPOX: acetic acid (red), hydroxyacetone (blue), glycolaldehyde (black), and formic acid (magenta).

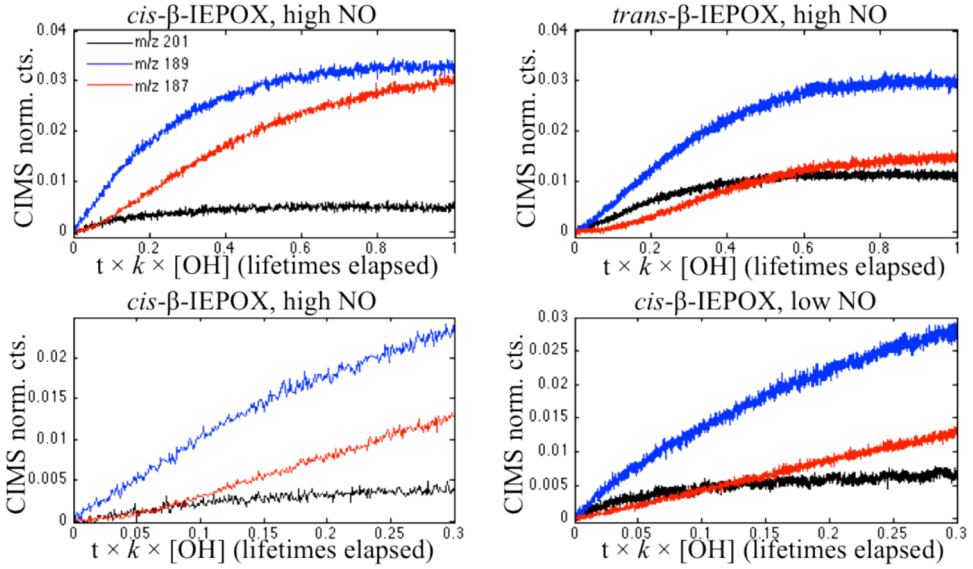


**Figure 5.** Time traces of dominant large products observed in the OH-initiated oxidation of *cis-β-* and *trans-β*-IEPOX: *m/z* 201 (black), 189 (blue), and 187 (red).

**Table 3. First-Generation Yields of Dominant Products from the Oxidation of *cis-β*-IEPOX and *trans-β*-IEPOX**

| | | yield (%) | | |
|---|---|---|---|---|
| compound | sensitivity[a] | *cis-β*-IEPOX, high NO | *cis-β*-IEPOX, low NO | *trans-β*-IEPOX, high NO |
| *m/z* 201 | variable[b] | 10.6 ± 0.7 | 12.9 ± 1.0 | 10.5 ± 0.27 |
| *m/z* 189 | variable[b] | 46.4 ± 1.7 | 37.1 ± 2.2 | 21.7 ± 0.5 |
| *m/z* 187 | variable[b] | 14.4 ± 0.6 | 10.4 ± 0.6 | 3.69 ± 0.15 |
| glycolaldehyde | $4.0 \times 10^{-4}$ | 11.8 ± 0.5 | 2.5 ± 0.6 | 4.55 ± 0.24 |
| hydroxyacetone | $3.8 \times 10^{-4}$ | 16.8 ± 0.3 | 8.5 ± 0.5 | 5.41 ± 0.17 |
| acetic acid | $2.3 \times 10^{-4}$ | 4.3 ± 0.3 | 7.8 ± 1.2 | 2.7 ± 0.3 |
| formic acid | $2.7 \times 10^{-4}$ | 15.8 ± 0.5 | 27.8 ± 2.1 | 8.8 ± 0.5 |

[a]In normalized counts per ppt in CIMS flow tube. [b]Sensitivities of large products were assumed to be equal to that of their parent IEPOX isomer: $4.0 \times 10^{-4}$ and $2.2 \times 10^{-4}$, respectively, for *cis-* and *trans-β*-IEPOX.

factors were determined in previous experiments.[23] For larger products without authentic standards, instrumental sensitivities were assumed to be equal to those of their parent IEPOX isomer, as estimated in previous work based on polarizability and dipole moments.[11,23] Yields were then calculated by determining the slope of a simple linear regression between the


dx.doi.org/10.1021/jp4107958 | J. Phys. Chem. A XXXX, XXX, XXX−XXX

mixing ratios of IEPOX and each product over the first 10−20 min of oxidation.

Time traces of oxidation products are shown in Figures 4 and 5, and first-generation product yields are given in Table 3. Reported uncertainties of yields account only for the standard deviations of the regressions, and do not include possible errors in calibration factors (estimated to be ±30% for hydroxyacetone and glycolaldehyde and ±20% for formic and acetic acids). Because these calibration factors have significant uncertainty and the CIMS sensitivity to IEPOX was not directly measured on the instruments used for these experiments, absolute yields cannot be accurately quantified, but yields can be compared between experiments. Additionally, because the yields reported in Table 3 are given as a percent of the IEPOX lost rather than as a percent of the total products observed, they do not necessarily add to 100%. Products lost to walls, products undetectable by our CIMS instruments, and uncertainty in sensitivity estimates all contribute to this deviation from carbon parity. We believe that uncertainties in the IEPOX and other large product sensitivity estimates account for the majority of error in the calculated yields, and for modeling purposes, we suggest scaling the yields to a sum of 100%, knowing that significant uncertainties will persist until a more accurate determination of product yields can be measured.

The dominant small products of IEPOX oxidation detected by CIMS (Figure 4) were formic acid (FA, monitored at $m/z$ 65 for FA·$F^-$), acetic acid (AA, $m/z$ 79 for AA·$F^-$), glycolaldehyde (GLYC, $m/z$ 145 for GLYC·$CF_3O^-$, corrected for AA·$CF_3O^-$), and hydroxyacetone (HAC, $m/z$ 159 for HAC·$CF_3O^-$). Under high-NO conditions, both *cis*-$\beta$- and *trans*-$\beta$-IEPOX produced nearly equivalent first-generation yields of glycolaldehyde and hydroxyacetone. This matches previous speculation on the oxidation mechanism of IEPOX, such as those used in SAPRC-07 and MCM 3.2.[34,35] Both isomers also produced significant levels of formic and acetic acids, which had not been previously reported in IEPOX oxidation. Low-NO oxidation of *cis*-$\beta$-IEPOX resulted in diminished first-generation yields of glycolaldehyde and hydroxyacetone and elevated yields of acetic and formic acids relative to oxidation under high-NO conditions, suggesting a strongly NO-dependent mechanism for the formation of these small products.

The most prevalent $C_4$−$C_5$ products detected by CIMS (Figure 5) appeared at $m/z$ 201, 189, and 187. Under high- and low-NO conditions, the two isomers gave nearly identical yields of the $m/z$ 201 product. In contrast, *cis*-$\beta$-IEPOX produced over twice as much of the $m/z$ 189 product as the trans isomer did, and nearly four times as much of the $m/z$ 187 product. This evidence, along with differences in the yields of small products between the isomers, suggests a stark disparity between the oxidation pathways of the two isomers. We do not currently have an explanation for this difference, but ongoing computational studies are expected to shed light on this intriguing chemistry. Additionally, the appearance of significant amounts of large products under high-NO conditions contrasts with the IEPOX oxidation mechanism used currently in photochemical models (e.g., MCM v3.2 and SAPRC07), in which IEPOX degrades quickly to form hydroxyacetone, glycolaldehyde, and other small products.[34] Low-NO oxidation of *cis*-$\beta$-IEPOX produced slightly less of the $m/z$ 189 and 187 products and slightly more of the $m/z$ 201 product than under high-NO conditions, but the small magnitude of these changes suggests only a minor NO dependence of this oxidation pathway.

Proposed structures for the $m/z$ 201, 189, and 187 compounds are shown in Figure 6. While many of these

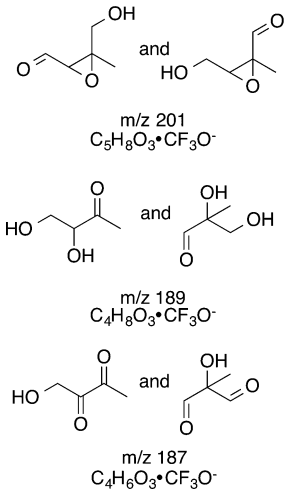


**Figure 6.** Proposed structures of the dominant large products observed in the OH-initiated oxidation of *cis*-$\beta$- and *trans*-$\beta$-IEPOX.

structures have been suggested previously as intermediates in the oxidative degradation of IEPOX, most have not yet been considered first-generation products, and their designation as such requires reconsideration of the mechanism for the first steps of IEPOX oxidation. We propose such a mechanism in Figure 7. We stress that this mechanism is neither complete nor certain, and it does not yet account for differing oxidation pathways between the two $\beta$-IEPOX isomers nor for the formation of formic and acetic acids, but it improves upon existing mechanisms by incorporating both previous insights and the present results.

The mechanism begins with hydrogen abstraction by OH at the 1, 3, or 4 position. In the case of abstraction at positions 1 or 4, addition of $O_2$ and subsequent elimination of $HO_2$ gives the $m/z$ 201 product, which accounts for ∼10% of the first-generation pathway. Alternatively, a series of rearrangements can form a more stable alkyl radical prior to $O_2$ addition. The resulting peroxy radical can then undergo a variety of possible transformations. Reaction with $HO_2$, NO, or $RO_2$ to form the alkoxy radical results in fragmentation of the molecule, forming either a $C_3$ and a $C_2$ product or a $C_4$ product and CO. These pathways account for the formation of hydroxyacetone, glycolaldehyde, and the product detected at $m/z$ 189. This mechanism also implies that glyoxal and methylglyoxal, neither of which can be detected by the CIMS instruments used here, are produced concurrently with hydroxyacetone and glycolaldehyde, respectively. Additionally, the peroxy radical can undergo unimolecular decomposition, via a 1,4-H shift from the $\alpha$ aldehyde or a 1,5-H shift from the $\alpha$ hydroxyl group, to form the same sets of products accessed by the alkoxy radical pathway. The product detected at $m/z$ 189 can further react with OH and $O_2$ to form products detectable at $m/z$ 187. Theoretically, the peroxy radical could also react with $HO_2$ to form a hydroperoxide or with NO to form a nitrate. Low product signal was observed at a mass consistent with the hydroperoxide (<5% under low-NO conditions), and almost no product was observed at a mass consistent with the nitrate (<1% under high-NO conditions), suggesting either that these reactions do not readily occur or that the nonvolatile products are quickly lost to chamber walls.


dx.doi.org/10.1021/jp4107958 | J. Phys. Chem. A XXXX, XXX, XXX−XXX

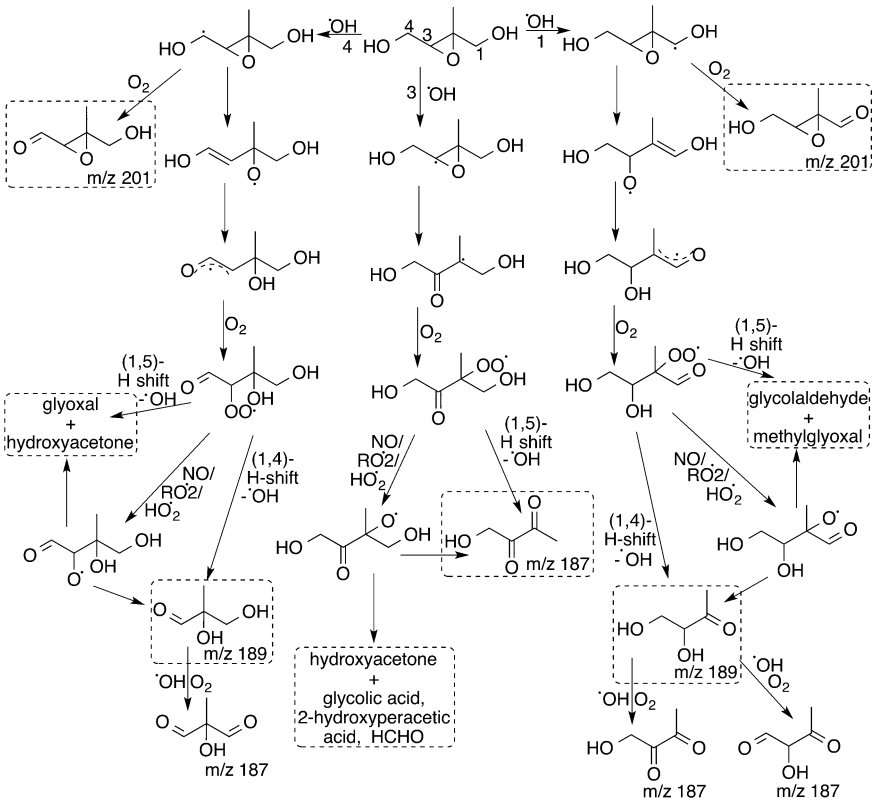


**Figure 7.** Proposed mechanism for the OH-initiated oxidation of $\beta$-IEPOX. Proposed first-generation products are outlined in dashed boxes.

In the case of hydrogen abstraction by OH at position 3, no product detectable at $m/z$ 201 can be formed. Instead, isomerization and addition of $O_2$ leads directly to the peroxy radical, which can again undergo a 1,5-H shift with the $\alpha$ hydroxyl group and decompose to form a $C_4$ fragment. The $C_4$ fragment produced by the H-shift mechanism differs from those produced by abstraction at positions 1 and 4, and accounts for the first-generation yield of the product detected at $m/z$ 187. Alternatively, the peroxy radical can react with $HO_2$, NO, or $RO_2$ to form the alkoxy radical, which decomposes to form either the same $C_4$ fragment or hydroxyacetone and a $C_2$ fragment. The $C_2$ fragment produced by this mechanism is expected to form glycolic or 2-hydroxyperacetic acids by reaction with $HO_2$ or decompose to formaldehyde.[34] Low product signal was observed at masses consistent with the two acids (<2%). The sum of the yields of $m/z$ 187 and hydroxyacetone provides an upper limit for the fraction of IEPOX + OH hydrogen abstraction that occurs at position 3, as hydroxyacetone can also be formed from other pathways. The yields reported in this study suggest that the first-generation formation of the $m/z$ 189 products is the dominant pathway of IEPOX oxidation and that hydrogen abstraction by OH occurs primarily at positions 1 and 4, but all pathways shown in Figure 7 contribute to the overall product breakdown of OH-initiated IEPOX degradation.

Many aspects of our proposed mechanism coincide with the scheme recently proposed by Elrod et al.[25] for *trans*-$\beta$-IEPOX, with the exception of our inclusion of the $m/z$ 189 and 187 products, which they did not observe. Setting aside these compounds, the relative yields of hydroxyacetone, glycolaldehyde, and the $m/z$ 201 product from *trans*-$\beta$-IEPOX oxidation are similar to those reported by Elrod et al. Their study also shows products that our CIMS would observe at $m/z$ 163, 217, and 235. With the exception of $m/z$ 235, of which we detect small yields (<5%) with low statistical significance, these products are not observed in our experiments.

## CONCLUSIONS

The recent discovery of IEPOX and evidence of its importance as an isoprene oxidation product and SOA precursor has led to widespread interest in its atmospheric fate. As IEPOX is estimated to account for a significant mass of global VOC ($\sim$100 Tg C $y^{-1}$), an understanding of its chemistry is critically important. The results presented here provide new insight into IEPOX behavior, which can be incorporated into chemical mechanisms of low-NO isoprene oxidation. The relative yields of IEPOX isomers as reported here, along with the OH oxidation rates of those isomers, serve to constrain the isomer distribution in the atmosphere and explain the isomeric yields of 2-methyltetrols found in SOA. As differences in oxidation pathways between IEPOX isomers are elucidated, isomer abundances will further improve estimates of product yields.

The product studies conducted in this investigation largely corroborate existing predictions of the IEPOX oxidation pathway. Major products observed at $m/z$ 189 and 187 fit with the existing MCM mechanism,[34] although they notably appear as first-generation products rather than subsequent intermediates. Atmospheric observations of these products in high-isoprene, low-NO environments would test this finding. Yields of smaller products also generally match predictions, with the exception of formic acid, which has a much higher yield than currently predicted. However, differences in yields of most products between the two $\beta$-IEPOX isomers suggest substantial divergence in the oxidation pathways for the two atmospherically dominant IEPOX isomers. Additionally, assuming glyoxal and methylglyoxal are coproducts of


dx.doi.org/10.1021/jp4107958 | J. Phys. Chem. A XXXX, XXX, XXX−XXX

hydroxyacetone and glycoaldehyde in the oxidation of IEPOX, this chemistry is likely important in closing some of the disagreement between simulated and observed levels of these compounds in isoprene-rich environments.[36,37] Although further studies incorporating measurements of glyoxal and methylglyoxal will be necessary to fully constrain the products of IEPOX oxidation and to reconcile differences between our experiments and those of Elrod et al.,[25] the products reported here provide a framework from which to improve existing models.

## ■ ASSOCIATED CONTENT

### Supporting Information

NMR spectra of synthesized IEPOX isomers. This material is available free of charge via the Internet at http://pubs.acs.org.

## ■ AUTHOR INFORMATION


### Corresponding Author

*(K.H.B.) E-mail: kelvin@caltech.edu.

### Present Address

‖(N.B.B.) Department of Chemistry, University of California Irvine, Irvine, California 92697, United States.


### Notes

The authors declare no competing financial interest.

## ■ ACKNOWLEDGMENTS

The authors would like to thank Prof. Jason D. Surratt for correspondence regarding the synthesis of IEPOX and the National Science Foundation (AGS 1240604) for their support of this research.

## ■ REFERENCES


(1) Guenther, A.; Karl, T.; Harley, P.; Wiedinmyer, C.; Palmer, P. I.; Geron, C. Estimates of Global Terrestrial Isoprene Emissions Using MEGAN (Model of Emissions of Gases and Aerosols from Nature). *Atmos. Chem. Phys.* **2006**, *6*, 3181−3210.

(2) Atkinson, R.; Baulch, D. L.; Cox, R. A.; Crowley, J. N.; Hampson, R. F.; Hynes, R. G.; Jenkin, M. E.; Rossi, M. J.; Troe, J. Evaluated Kinetic and Photochemical Data for Atmospheric Chemistry: Volume 2: Reactions of Organic Species. *Atmos. Chem. Phys.* **2006**, *6*, 3625−4055.

(3) Rosenstiel, T.; Potosnak, M.; Griffin, K.; Fall, R.; Monson, R. Increased $CO_2$ Uncouples Growth from Isoprene Emission in an Agriforest Ecosystem. *Nature* **2003**, *421*, 256−259.

(4) Wiedinmyer, C.; Tie, X.; Guenther, A.; Neilson, R.; Granier, C. Future Changes in Biogenic Isoprene Emissions: How Might They Affect Regional and Global Atmospheric Chemistry? *Earth Interact.* **2006**, *10*, 1−19.

(5) Kuhlmann, R. V.; Lawrence, M. G. Sensitivities in Global Scale Modeling of Isoprene. *Atmos. Chem. Phys.* **2004**, *4*, 1−17.

(6) Crutzen, P. J.; Williams, J.; Po, U.; Hoor, P.; Fischer, H.; Warneke, C.; Holzinger, R.; Hansel, A.; Lindinger, W.; Scheeren, B.; et al. High Spatial and Temporal Resolution Measurements of Primary Organics and their Oxidation Products over the Tropical Forests of Suriname. *Atmos. Environ.* **2000**, *34*, 1161−1165.

(7) Lelieveld, J.; Butler, T. M.; Crowley, J. N.; Dillon, T. J.; Fischer, H.; Ganzeveld, L.; Harder, H.; Lawrence, M. G.; Martinez, M.; Taraborrelli, D.; et al. Atmospheric Oxidation Capacity Sustained by a Tropical Forest. *Nature* **2008**, *452*, 737−740.

(8) Ren, X.; Olson, J. R.; Crawford, J. H.; Brune, W. H.; Mao, J.; Long, R. B.; Chen, Z.; Chen, G.; Avery, M. A.; Sachse, G. W.; et al. $HO_x$ Chemistry during INTEX-A 2004: Observation, Model Calculation, and Comparison with Previous Studies. *J. Geophys. Res.* **2008**, *113*, D05310.

(9) Liu, Y. J.; Herdlinger-Blatt, I.; McKinney, K. A.; Martin, S. T. Production of Methyl Vinyl Ketone and Methacrolein via the Hydroperoxyl Pathway of Isoprene Oxidation. *Atmos. Chem. Phys.* **2013**, *13*, 5715−5730.

(10) Navarro, M. A.; Dusanter, S.; Hites, R. A.; Stevens, P. S. Radical Dependence of the Yields of Methacrolein and Methyl Vinyl Ketone from the OH-Initiated Oxidation of Isoprene under $NO_x$-free Conditions. *Environ. Sci. Technol.* **2011**, *45*, 923−929.

(11) Paulot, F.; Crounse, J. D.; Kjaergaard, H. G.; Kürten, A.; St Clair, J. M.; Seinfeld, J. H.; Wennberg, P. O. Unexpected Epoxide Formation in the Gas-Phase Photooxidation of Isoprene. *Science* **2009**, *325*, 730−733.

(12) Thornton, J. A.; Wooldridge, P. J.; Cohen, R. C.; Martinez, M.; Harder, H.; Brune, W. H.; Williams, E. J.; Roberts, J. M.; Fehsenfeld, F. C.; Hall, S. R.; et al. Ozone Production Rates as a Function of $NO_x$ Abundances and $HO_x$ Production Rates in the Nashville Urban Plume. *J. Geophys. Res.* **2002**, *107* (D12), ACH 7−1−ACH 7−17.

(13) Surratt, J. D.; Murphy, S. M.; Kroll, J. H.; Ng, N. L.; Hildebrandt, L.; Sorooshian, A.; Szmigielski, R.; Vermeylen, R.; Maenhaut, W.; Claeys, M.; et al. Chemical Composition of Secondary Organic Aerosol Formed from the Photooxidation of Isoprene. *J. Phys. Chem. A* **2006**, *110*, 9665−9690.

(14) Surratt, J. D.; Chan, A. W. H.; Eddingsaas, N. C.; Chan, M.; Loza, C. L.; Kwan, A. J.; Hersey, S. P.; Flagan, R. C.; Wennberg, P. O.; Seinfeld, J. H. Reactive Intermediates Revealed in Secondary Organic Aerosol Formation from Isoprene. *Proc. Natl. Acad. Sci. U.S.A.* **2010**, *107*, 6640−6645.

(15) Lin, Y.-H.; Zhang, Z.; Docherty, K. S.; Zhang, H.; Budisulistiorini, S. H.; Rubitschun, C. L.; Shaw, S. L.; Knipping, E. M.; Edgerton, E. S.; Kleindienst, T. E.; et al. Isoprene Epoxydiols as Precursors to Secondary Organic Aerosol Formation: Acid-Catalyzed Reactive Uptake Studies with Authentic Compounds. *Environ. Sci. Technol.* **2012**, *46*, 250−258.

(16) Nguyen, T. B.; Coggon, M. M.; Bates, K. H.; Zhang, X.; Schwantes, R. H.; Schilling, K. A.; Loza, C. L.; Flagan, R. C.; Wennberg, P. O.; Seinfeld, J. H. Organic Aerosol Formation from the Reactive Uptake of Isoprene Epoxydiols (IEPOX) onto Non-acidified Inorganic Seeds. *Atmos. Chem. Phys. Discuss.* **2013**, *13*, 27677−27716.

(17) Zhang, Z.-S.; Engling, G.; Chan, C.-Y.; Yang, Y.-H.; Lin, M.; Shi, S.; He, J.; Li, Y.-D.; Wang, X.-M. Determination of Isoprene-Derived Secondary Organic Aerosol Tracers (2-Methyltetrols) by HPAEC-PAD: Results from Size-Resolved Aerosols in a Tropical Rainforest. *Atmos. Environ.* **2013**, *70*, 468−476.

(18) Ding, X.; Zheng, M.; Yu, L.; Zhang, X.; Weber, R. J.; Yan, B.; Russell, A. G.; Edgerton, E. S.; Wang, X. Spatial and Seasonal Trends in Biogenic Secondary Organic Aerosol Tracers and Water-Soluble Organic Carbon in the Southeastern United States. *Environ. Sci. Technol.* **2008**, *42*, 5171−5176.

(19) Xia, X.; Hopke, P. K. Seasonal Variation of 2-Methyltetrols in Ambient Air Samples. *Environ. Sci. Technol.* **2006**, *40*, 6934−6937.

(20) Schkolnik, G.; Falkovich, A. H.; Rudich, Y.; Maenhaut, W.; Artaxo, P. A New Method for the Determination of Levoglucosan, Methyl-Erythritol and Related Compounds and Its Application for Rainwater and Smoke Samples. *Environ. Sci. Technol.* **2005**, *39*, 2744−2752.

(21) Claeys, M.; Graham, B.; Vas, G.; Wang, W.; Vermeylen, R.; Pashynska, V.; Cafmeyer, J.; Guyon, P.; Andreae, M. O.; Artaxo, P.; et al. Formation of Secondary Organic Aerosols through Photooxidation of Isoprene. *Science* **2004**, *303*, 1173−1176.

(22) Kourtchev, I.; Ruuskanen, T.; Maenhaut, W.; Kulmala, M.; Claeys, M. Observation of 2-Methyltetrols and Related Photooxidation Products of Isoprene in Boreal Forest Aerosols from Hyytiälä, Finland. *Atmos. Chem. Phys.* **2005**, *5*, 2761−2770.

(23) Paulot, F.; Crounse, J. D.; Kjaergaard, H. G.; Kroll, J. H.; Seinfeld, J. H.; Wennberg, P. O. Isoprene Photooxidation: New Insights into the Production of Acids and Organic Nitrates. *Atmos. Chem. Phys.* **2009**, *9*, 1479−1501.

(24) Xie, Y.; Paulot, F.; Carter, W. P. L.; Nolte, C. G.; Luecken, D. J.; Hutzell, W. T.; Wennberg, P. O.; Cohen, R. C.; Pinder, R. W.

Understanding the Impact of Recent Advances in Isoprene Photooxidation on Simulations of Regional Air Quality. *Atmos. Chem. Phys.* **2013**, *13*, 8439−8455.
(25) Elrod, M. J.; Jacobs, M. I.; Darer, A. D. Rate Constants and Products of the OH Reaction with Isoprene-Derived Epoxides. *Environ. Sci. Technol.* **2013**, *47*, 12868−12876.
(26) Zhang, Z.; Lin, Y.-H.; Zhang, H.; Surratt, J. D.; Ball, L. M.; Gold, A. Technical Note: Synthesis of Isoprene Atmospheric Oxidation Products: Isomeric Epoxydiols and the Rearrangement Products of *cis*- and *trans*-3-Methyl-3,4-dihydroxytetrahydrofuran. *Atmos. Chem. Phys.* **2012**, *12*, 8529−8535.
(27) Nefkens, G.; Thuring, J. W.; Zwanenburg, B. A Novel and Convenient Synthesis of 3-Methylfuran-2(5*H*)-one. *Synthesis* **1997**, *3*, 290−292.
(28) Hoang, T.; Lauher, J. W.; Fowler, F. W. The Topochemical 1,6-Polymerization of a Trieme. *J. Am. Chem. Soc.* **2002**, *124*, 10656−10657.
(29) St. Clair, J. M.; McCabe, D. C.; Crounse, J. D.; Steiner, U.; Wennberg, P. O. Chemical Ionization Tandem Mass Spectrometer for the in Situ Measurement of Methyl Hydrogen Peroxide. *Rev. Sci. Instrum.* **2010**, *81*, 94−102.
(30) Crounse, J. D.; McKinney, K. A.; Kwan, A. J.; Wennberg, P. O. Measurement of Gas-Phase Hydroperoxides by Chemical Ionization Mass Spectrometry. *Anal. Chem.* **2006**, *78*, 6726−6732.
(31) Atkinson, R.; Arey, J. Atmospheric Degradation of Volatile Organic Compounds. *Chem. Rev.* **2003**, *103*, 4605−4638.
(32) York, D.; Evensen, N.; Martinez, M.; Delgado, J. Unified Equations for the Slope, Intercept, and Standard Errors of the Best Straight Line. *Am. J. Phys.* **2004**, *72*, 367−375.
(33) Eddingsaas, N. C.; VanderVelde, D. G.; Wennberg, P. O. Kinetics and Products of the Acid-Catalyzed Ring-Opening of Atmospherically Relevant Butyl Epoxy Alcohols. *J. Phys. Chem. A* **2010**, *114*, 8106−8113.
(34) Saunders, S. M.; Jenkin, M. E.; Derwent, R. G.; Pilling, M. J. Protocol for the Development of the Master Chemical Mechanism, MCM v3 (Part A): Tropospheric Degradation of Non-Aromatic Volatile Organic Compounds. *Atmos. Chem. Phys.* **2003**, *3*, 161−180.
(35) Carter, W. P. L. Development of the SAPRC-07 Chemical Mechanism. *Atmos. Environ.* **2010**, *44*, 5324−5335.
(36) Myriokefalitakis, S.; Vrekoussis, M.; Tsirigaridis, K.; Wittrock, F.; Richter, A.; Brühl, C.; Volkamer, R.; Burrows, J. P.; Kanakidou, M. The Influence of Natural and Anthropogenic Secondary Sources on the Glyoxal Global Distribution. *Atmos. Chem. Phys.* **2008**, *8*, 4965−4981.
(37) Wittrock, F.; Richter, A.; Oetjen, H.; Burrows, J. P.; Kanakidou, M.; Myriokefalitakis, S.; Volkamer, R.; Beirle, S.; Platt, U.; Wagner, T. Simultaneous Global Observations of Glyoxal and Formaldehyde from Space. *Geophys. Res. Lett.* **2006**, *33*, L16804.